Available online at www.sciencedirect.com
SCIENCE DIRECT®
ELSEVIER
Bioorganic & Medicinal Chemistry 12 (2004) 257–264
Bioorganic & Medicinal Chemistry

Relationships between structure and high-throughput screening permeability of peptide derivatives and related compounds with artificial membranes: application to prediction of Caco-2 cell permeability

Rieko Ano, Yukitaka Kimura, Motohiro Shima, Ryuichi Matsuno, Tamio Ueno and Miki Akamatsu*

Graduate School of Agriculture, Kyoto University, Kyoto 606-8502, Japan

Received 21 August 2003; accepted 1 October 2003

Abstract—To evaluate absorption of compounds across the membrane via a transcellular route, the permeability of peptide derivatives and related compounds was measured by the parallel artificial membrane permeation assay (PAMPA). The permeability coefficients by PAMPA were analyzed quantitatively using classical QSAR and Volsurf approaches with the physicochemical parameters. The results from both approaches showed that hydrogen bonding ability of molecules in addition to hydrophobicity at a particular pH were significant in determining variations in PAMPA permeability coefficients. The relationship between Caco-2 cell permeability and artificial lipid membrane permeability was then determined. The compounds were sorted according to their absorption pathway in the plot of the Caco-2 cell and PAMPA permeability coefficients.

1. Introduction

The molecular properties for absorption, distribution, metabolism, and excretion (ADME) are crucial for drug design. It has been recognized that prediction of ADME properties is important at the initial step of drug development. A number of models for predicting oral drug absorption have been developed in recent years.[1–19] Peptidomimetics which are designed to enhance the oral absorption of bioactive peptides and depress their enzymatic degradation can be good candidates of drugs. Therefore, clarifying structural factors of peptides and their derivatives which influence their epithelial permeation and metabolism should provide information for the design of peptidomimetics.

Good correlation between oral drug absorption in humans and apparent permeability coefficients of drugs in Caco-2 cells, the cell line derived from human colon carcinoma, have been reported.[20] Caco-2 cells express transporters such as PEPT1,[21] a peptide transporter, and an efflux system, P-glycoprotein (P-gp).[22] Previously, we reported the permeability, possible transport mechanism, and metabolism of peptide derivatives containing Trp and related compounds across human intestinal epithelial (Caco-2) cells.[23] Most peptide derivatives were hydrolysed not only by the cytosolic enzymes in Caco-2 cells during permeation but also by enzymes released to the apical solution before cell permeation. We also observed that N-terminal blocked dipeptides were more resistant to hydrolases expressed in the Caco-2 cells and that indole derivatives were not entirely degraded. We also demonstrated that zwitterionized peptides and peptide amides were mainly transported by active transporters whereas N-terminal protected and cyclic peptides were passively transported. A few compounds were indicated to be excreted by P-gp. However, it is difficult to determine which structural features of the compounds will be responsible for interaction with the transporters because multiple transporters are expressed in Caco-2 cells. Although Caco-2 cells are a useful model system to evaluate metabolism and absorption of compounds, understanding the role of passive transport phenomena are also important. In addition, the method using Caco-2

Keywords: PAMPA; Artificial membrane; Caco-2; Structure–permeability relationships; Dipeptide derivatives; Indole compounds.
* Corresponding author. Tel./fax: +81-75-753-6489; e-mail: akamatsu@kais.kyoto-u.ac.jp

0968-0896/$ - see front matter © 2003 Elsevier Ltd. All rights reserved.
doi:10.1016/j.bmc.2003.10.002

cells is rather labor-intensive and not easily applicable for high-throughput screening.

Recently, the parallel artificial membrane permeation assay (PAMPA) was proposed by Kansy et al.[24] PAMPA is a rapid in vitro assay, which is applicable for high-throughput, consisting of hydrophobic filters coated with a lecithin in organic solvent solution. The modified methods of PAMPA were also reported by Sugano et al.[25,26] and Wohnsland and Faller.[27] These methods were shown to enable prediction of absorption by passive transcellular pathway.[25–27]

In this study, the artificial lipid membrane permeability of peptide derivatives and related compounds was measured by PAMPA, in order to evaluate absorption of the compounds across the membrane by the transcellular route. Initially we quantitatively analyzed the permeability by PAMPA using classical QSAR and VolSurf[1,28] approaches with the physicochemical parameters such as hydrophobicity, pK_a and hydrogen-bond potential and so on, to simply predict passive absorption from the structure of compounds. The relationship between the Caco-2 cell and artificial lipid membrane permeability was then determined.

2. Results

2.1. Permeability with artificial membranes

The log $P_{\text{app-pampa}}$ values, $P_{\text{app-pampa}}$ being the permeability coefficient through the artificial membrane, at pH 6.3 and 7.3 are listed in Table 1. The $P_{\text{app-pampa}}$ values ranged from 0.12 to 31.91 $\times 10^{-6}$ cm/s. Although we attempted to measure $P_{\text{app-pampa}}$ values of zwitterionized dipeptides and *N*-acetyl dipeptides, it was difficult to obtain reliable values because the permeability of the compounds was too low ($<10^{-7}$ cm/s).

2.2. Classical quantitative structure–activity relationships (QSARs) for the log $P_{\text{app-pampa}}$

We quantitatively analyzed the PAMPA permeability, log $P_{\text{app-pampa}}$, using the physicochemical parameters of the compounds, log P_{oct} in 1-octanol/water system, the absolute value of the difference between the pK_a value of the compound and the experimental pH, $|\text{p}K_a - \text{pH}|$, and the surface area occupied by hydrogen bond donor and acceptor atoms, SA_{HD} and SA_{HA}, respectively. Eqs 1 and 2 were obtained with the same parameters for the both analyses of the permeability coefficients at pH 6.3 and 7.3.

At pH 6.3

$$\begin{aligned}\log P_{\text{app-pampa}} &= 0.51(\pm0.13)\log P_{\text{oct}} - 0.19(\pm0.13) \\ &\quad \times |\text{p}K_a - \text{pH}| - 2.18(\pm0.73)SA_{\text{HA}} \\ &\quad - 5.18(\pm0.38) \\ n = 22 \quad s = 0.28 \quad r^2 &= 0.85\end{aligned} \tag{1}$$

At pH 7.3

$$\begin{aligned}\log P_{\text{app-pampa}} &= 0.56(\pm0.15)\log P_{\text{oct}} - 0.27(\pm0.12) \\ &\quad \times |\text{p}K_a - \text{pH}| - 2.34(\pm0.70)SA_{\text{HA}} \\ &\quad - 5.14(\pm0.36) \\ n = 22 \quad s = 0.27 \quad r^2 &= 0.85\end{aligned} \tag{2}$$

In eq 1 and the following correlation equations, n is the number of compounds, s is the standard deviation, r is the correlation coefficients, and the figures in parentheses are the 95% confidence intervals. SA_{HD} was not significant in eqs 1 and 2. Eqs 1 and 2 indicate that the higher log P_{oct} and the closer pK_a to the experimental pH, the higher membrane permeability the compound has. Furthermore, the larger surface area occupied by hydrogen bond acceptor atoms is unfavorable for the permeation through membranes.

2.3. VolSurf analyses

The same log $P_{\text{app-pampa}}$ dataset was statistically analyzed by Partial Least Squares (PLS) method using the software, VolSurf,[28] which was developed as a three-dimensional QSAR procedure for predicting ADME properties of a molecule. Eqs 3 and 4 having good statistical quality were obtained. The PLS coefficient of variables in eq 3 was graphed in Figure 1. The coefficient of variables in eq 4 was similar to that in eq 3 (figure not shown).

At pH 6.3

$$\begin{aligned}\log P_{\text{app-pampa}} &= \text{VolSurf parameters} - 5.680 \\ &\text{Component Number} = 4, \quad n = 22, \\ &SE_{\text{calc}} = 0.24, \quad r^2 = 0.89, \\ &SE_{\text{pred}} = 0.49, \quad r^2_{\text{pred}} = 0.55\end{aligned} \tag{3}$$

At pH 7.3

$$\begin{aligned}\log P_{\text{app-pampa}} &= \text{VolSurf parameters} - 5.753 \\ &\text{Component Number} = 4, \quad n = 22, \\ &SE_{\text{calc}} = 0.26, \quad r^2 = 0.87, \\ &SE_{\text{pred}} = 0.43, \quad r^2_{\text{pred}} = 0.65\end{aligned} \tag{4}$$

Figure 1 indicates that the larger hydrophilic regions and hydrogen bonding ability, the lower membrane permeability. On the other hand, the larger hydrophobic regions, the higher permeability as expected. Factors such as size and shape increased membrane permeability of compounds. In general, integy moments and hydrophobic integy moments[28] that are vectors pointing from

Table 1. Permeability coefficients of peptide derivatives and related compounds, and QSAR parameters

No.		Compd	$P_{app\text{-}pampa}$ ($\times10^{-6}$)[a] (cm/s)		log $P_{app\text{-}pampa}$		$P_{app\text{-}Caco2}$ ($\times10^{-6}$)[b]	log $P_{app\text{-}Caco2}$	log P_{oct}	SA_{HA}[c]	SA_{HD}[d]	pK_a−6.3	pK_a−7.3
			pH 6.3	pH 7.3	pH 6.3	pH 7.3							
1	Trp derivatives	Boc-Trp	4.30 (0.35)	1.84 (0.99)	−5.37	−5.74	2.15	−5.67	2.65[e]	0.557	0.438	−2.6[f]	−3.6[f]
2		Cbz-Trp	7.13 (0.36)	2.82 (0.95)	−5.15	−5.55	1.58	−5.80	3.20[e]	0.637	0.439	−2.6[f]	−3.6[f]
3		Fmoc-Trp	11.65 (0.94)	12.75 (1.36)	−4.93	−4.89	17.45	−4.76	4.93[e]	0.658	0.439	−2.6[f]	−3.6[f]
4		Trp-NH_2	1.88 (0.33)	2.73 (0.27)	−5.73	−5.56	12.08	−4.92	0.30[e]	0.320	0.661	1.2[g]	0.2[g]
5		Ac-Trp-NH_2	2.51 (0.45)	1.92 (0.36)	−5.60	−5.72	2.35	−5.63	0.42[e]	0.419	0.488	0.0	0.0
6	X-Trp-NH_2	Gly-Trp-NH_2	0.14 (0.10)	0.42 (0.21)	−6.86	−6.38	6.67	−5.18	−0.48	0.530	0.832	0.4[h]	0.0
7		Phe-Trp-NH_2	3.13 (0.29)	5.98 (0.61)	−5.50	−5.22	10.45	−4.98	1.38	0.513	0.833	0.4[h]	0.0
8		Trp-Ala-Val-NH_2	0.23 (0.08)	0.24 (0.05)	−6.64	−6.62	n.d.	—	0.40	0.663	0.930	0.4[h]	0.0
9	Ac-dipeptide-NH_2	Ac-Trp-Val-NH_2	1.21 (0.12)	0.66 (0.48)	−5.92	−6.18	0.17	−6.77	0.73[i]	0.635	0.685	0.0	0.0
10		Ac-D-Trp-Val-NH_2	1.83 (0.43)	0.73 (0.73)	−5.74	−6.14	0.12	−6.92	0.65	0.541	0.643	0.0	0.0
11		Ac-Tyr-Leu-NH_2	0.19 (0.15)	0.29 (0.11)	−6.72	−6.54	n.d.	—	0.32[i]	0.527	0.657	0.0	0.0
12		Ac-Tyr-Phe-NH_2	0.33 (0.16)	0.12 (0.10)	−6.48	−6.92	n.d.	—	0.54[i]	0.713	0.668	0.0	0.0
13	Cyclo(Trp-X)	Cyclo(Trp-Gly)	0.34 (0.15)	0.97 (0.70)	−6.47	−6.02	0.76	−6.12	0.07	0.509	0.452	0.0	0.0
14		Cyclo(Trp-Tyr)	0.56 (0.30)	0.68 (0.70)	−6.25	−6.17	n.d.	—	1.11	0.621	0.580	0.0	0.0
15		Cyclo(Trp-Trp)	9.66 (0.99)	9.10 (1.99)	−5.01	−5.04	1.21	−5.92	2.04	0.533	0.586	0.0	0.0
16	Indole derivatives	Indole	25.71 (6.87)	31.91 (7.17)	−4.59	−4.50	57.33	−4.24	2.14[j]	0.079	0.149	0.0	0.0
17		Tryptophol	16.95 (0.81)	19.11 (2.02)	−4.77	−4.72	57.49	−4.24	1.54	0.196	0.295	0.0	0.0
18		Tryptamine	2.95 (0.25)	5.42 (1.24)	−5.53	−5.27	n.d.	—	1.35[j]	0.124	0.427	3.9[k]	2.9[k]
19		Indole-3-acetamide	7.21 (0.37)	6.18 (0.56)	−5.14	−5.21	59.01	−4.23	0.75	0.280	0.414	0.0	0.0
20		Indole-3-carboxylic acid	3.10 (0.06)	0.79 (0.05)	−5.51	−6.10	27.46	−4.56	1.99[j]	0.398	0.291	−2.1[l]	−3.1[l]
21		Indole-3-acetic acid	1.38 (0.03)	0.40 (0.02)	−5.86	−6.40	14.16	−4.85	1.41[j]	0.362	0.279	−2.0[m]	−3.0[m]
22		Indole-3-propionic acid	6.36 (0.39)	2.10 (0.73)	−5.20	−5.68	21.30	−4.67	1.75[j]	0.366	0.290	−1.6[n]	−2.6[n]

[a] The measurement was repeated at least four times. Values in parentheses are the standard deviation.
[b] Caco-2 permeability coefficients. From refs 23 and 30.
[c] Van der Waals surface area (Å^2 × 1/100) occupied by hydrogen-bond acceptor atoms.
[d] Van der Waals surface area (Å^2 × 1/100) occupied by hydrogen-bond donor atoms.
[e] From ref 30.
[f] Calculated from the pK_a value of Ac-Ala (3.7[43]).
[g] Calculated from the pK_a value of Trp-NH_2 (7.5[44]).
[h] Calculated from the pK_a value of Phe-Gly-NH_2 (6.7[44]).
[i] From ref 31.
[j] From ref 33.
[k] Calculated from the pK_a value of tryptamine (10.2[44]).
[l] Calculated from the pK_a value of benzoic acid (4.2[43]).
[m] Calculated from the pK_a value of phenylacetic acid (4.3[43]).
[n] Calculated from the pK_a value of 3-phenylpropionic acid (4.7[43]).

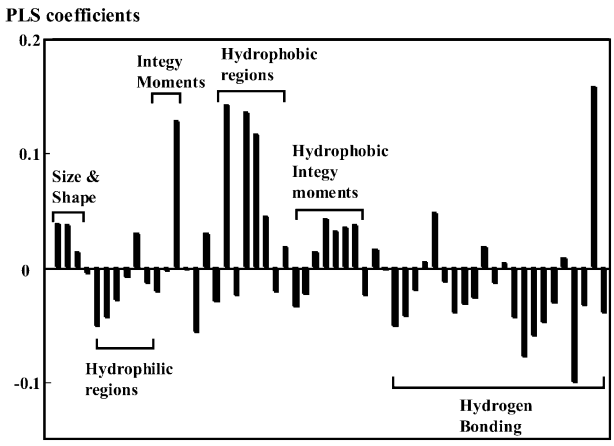

Figure 1. The PLS coefficient of variables in eq 3.

the center of the mass to the center of hydrophilic and hydrophobic regions, respectively, also increased the permeability.

3. Discussion

In this study, the relationship between permeability across artificial lipid membranes and the physicochemical parameters of the peptides and related compounds was investigated using classical QSAR and VolSurf approaches. In classical QSAR eqs 1 and 2, the coefficients of the corresponding terms and the intercept are identical within 95% confidence intervals, indicating the presence of the same absorption mechanism regardless of pH. As described in the experimental section, the term of $(\log P_{\mathrm{oct}} + |\mathrm{p}K_{\mathrm{a}} - \mathrm{pH}|)$ is equal to log D_{oct}, where D_{oct} is the distribution coefficient of compounds at a particular pH, for acids and bases if the partition of ion-pair complexes can be neglected. Therefore, the first log P_{oct} and second $|\mathrm{p}K_{\mathrm{a}} - \mathrm{pH}|$ terms in eqs 1 and 2 are considered to correspond to the apparent hydrophobicity at the pH. However, the result that the coefficients of the $|\mathrm{p}K_{\mathrm{a}} - \mathrm{pH}|$ term are significantly smaller than those of the log P_{oct} term suggests that a portion of the ion form of compounds may permeate across the artificial membrane.

Both classical QSAR and VolSurf equations gave similar results. The larger apparent hydrophobicity at a particular pH is favorable for permeation across the membrane whereas the higher hydrogen bonding capability of compounds is unfavorable for permeation. However, in classical QSAR, only the hydrogen accepting capability was significant whereas in VolSurf, both hydrogen accepting and donating capability of compounds seemed to take part in membrane permeation. Fujita et al. generalized the following equation for partition coefficients in different solvents from 1-octanol and water system.[29]

$$\log P_{\mathrm{solv}} = \log P_{\mathrm{oct}} + \Delta\log f(\mathrm{HB}) + \mathrm{const.} \quad (5)$$

$$\Delta\log f(\mathrm{HB}) = \log\left[f(\mathrm{HB})_{\mathrm{solv}}/f(\mathrm{HB})_{\mathrm{oct}}\right] \quad (6)$$

The f(HB) term is formulated with solvent molarity and the association equilibrium constant for compounds and a solvent. Thus, the $\Delta\log f$(HB) term relates to the difference of the hydrogen bonding capability of compounds for a solvent and 1-octanol. The SA_{HA} terms in eqs 1 and 2 correspond to the $\Delta\log f$(HB) term in eqs 5 and 6. Since both octanol and the artificial membrane (lecithin solution in 1,9-decadiene) have an amphiprotic character, it is not easy to theoretically determine if either hydrogen accepting or donating ability, or both give(s) the extra effect on the artificial membrane permeation when log P_{oct} is used as the reference to estimate the hydrophobicity. Further studies using compounds having more diverse structures is needed to discuss the role of hydrogen donors for permeation.

Previously, we reported the permeability coefficients of Trp and peptide derivatives, and related compounds across Caco-2 cells, the cell line derived from human colon carcinoma.[23,30] The compounds were classified into three classes according to their main absorption mechanism across Caco-2 cells; (1) passively transported compounds, (2) actively transported compounds and (3) compounds excreted by P-gp. The N-terminal blocked dipeptides; Ac-Trp-X, Ac-dipeptide-NH_2, cyclo(Trp-Gly), and the indole compounds; indole, indole-2-carboxylic acid, and tryptophol are included in group (1). The zwitterionized dipeptides; Trp-X and X-Trp, the peptide amides; X-Trp-NH_2, and the indole compounds; 3-methylindole, indole-3-acetic acid, indole-3-propionic acid, indole-3-butyric acid, indole-3-carboxylic acid, indole-3-carboxyaldehyde and indole-3-acetamide are categorized in group (2). Cyclo(Trp-Trp), Ac-Trp-Val-NH_2, and Ac-D-Trp-Val-NH_2 are likely to be included in group (3).

The relationship between the Caco-2 cell permeability coefficient from the apical to basolateral direction and the artificial membrane permeability coefficient at pH 7.3 is shown in Figure 2. Although it was difficult to obtain reliable $P_{\mathrm{app\text{-}pampa}}$ values of zwitterionized dipeptides and N-acetyl dipeptides because of their low permeability ($<10^{-7}$ cm/s), we added them to the plot of Figure 2 assuming their log $P_{\mathrm{app\text{-}pampa}} = -7$. The Caco-2 cell permeability coefficient, $P_{\mathrm{app\text{-}Caco\text{-}2}}$ of the compounds in group (1) except for N-acetyl dipeptides nicely correlated with their permeability coefficient by PAMPA, $P_{\mathrm{app\text{-}pampa}}$ ($r^2 = 0.98$), validating artificial membrane permeability as a simple effective model for passive transcellular transport. As shown in Figure 2, compounds in group (2) were positioned above the correlation line while compounds in group (3) were positioned below the correlation line. It is of interest that zwitterionized dipeptides, which are considered as substrates of a peptide active transporter PEPT1, were positioned above the correlation line as expected, while N-acetyl dipeptides passively transported were on elongation of the line even if their PAMPA permeability coefficients were based on the assumed log $P_{\mathrm{app\text{-}pampa}}$.

Several models for predicting oral drug absorption have been developed using either experimental or computational approaches.[2–4,15,18,19] Since apparent drug

permeability coefficients in Caco-2 cells is known to show good correlation with oral absorption of drugs in humans,[20] a number of predictive models of Caco-2 cell permeability have been also reported.[1,5–18] Lipinski's 'rule of five' predicted poor absorption for compounds based on characteristics such as molecular weight, hydrogen-bond donors and acceptors, and calculated hydrophobicity.[5] Ren and Lien proposed classical QSAR models for Caco-2 cell permeability using log D_{oct} at pH 7.4, molecular weight, intra-molecular hydrogen-bonding, and an indicator variable for charge.[8] Stenberg et al. indicated linear combinations of the dynamic average of polar and non-polar molecular surface areas for predicting intestinal drug permeability were important.[10] Neural network[12] and 3-D-QSAR techniques,[31] were also predictive for Caco-2 cell permeability. However, in some of these previous studies permeability coefficient values only of passively transported compounds through membranes were selected from experimentally measured values and analyzed. In the other studies, permeability coefficients were measured under conditions where active transport was reduced by the addition of inhibitors. In this situation, permeation by passive transport is mainly considered. In this study, we compared the compounds that are transported by various absorption mechanisms and the compounds were nicely sorted according to their absorption pathway as shown in Figure 2. Although the passive transcellular route may be dominant for drug transport across the intestinal epithelium,[10] active transport mechanisms including the P-gp efflux system likely play a role in both Caco-2 cells and in humans, as the case of the zwitterionized peptides shown in Figure 2. Contribution by each transport mechanism to the total permeability of compounds should be separately considered.

PAMPA is a good high-throughput screening system to evaluate the permeability by the passive transcellular route. Sugano et al. constructed a bio-(intestinal)-mimic lipid system mixing several lipids[25,26] and investigated

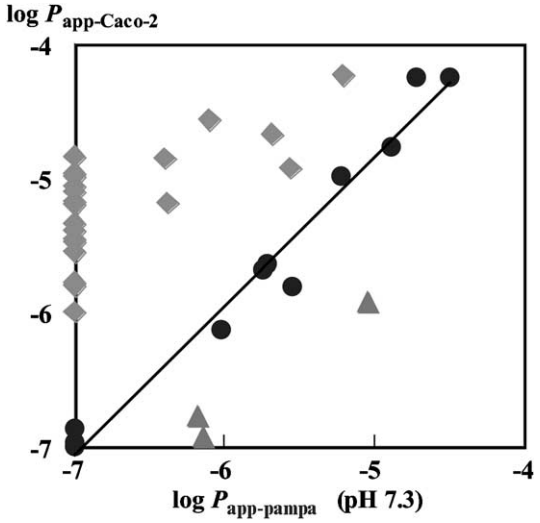

Figure 2. The relationship between the Caco-2 cell and artificial membrane permeability coefficients of compounds included in the group (1) (●), group (2) (◆), group (3) (▲).

correlation between the permeation of a variety of drugs using the system and oral absorption of the drugs in humans. Although their model seems to predict passive intestinal absorption in humans, the use of lipid mixtures makes it somewhat difficult to reproduce the permeability coefficients with good precision. Zhu et al. showed the relationship between PAMPA and Caco-2 cell permeability coefficients of a variety of drugs.[18] Since passive transcellular transport played an essential role in the absorption of most drugs they used, good correlation between their two permeabilities was obtained ($r^2 = 0.67$). However, no explanation based on the absorption mechanism was done for the deviated compounds from the correlation line in the paper.[18] Our study is the first attempt to quantitatively analyze PAMPA permeablilty and to show the predictive value of Caco-2 cell permeability coefficients using PAMPA with a single lipid.

4. Conclusion

Classical QSAR and VolSurf equations predicted PAMPA permeability, which evaluates the permeability of oligopeptide derivatives and related compounds via the passive transcellular route. In addition a plot of Caco-2 versus PAMPA permeability coefficients showed compounds were sorted according to their absorption pathway. The results should be useful for the design of orally-available peptidomimetic drugs.

5. Experimental

5.1. Materials

Peptides and their derivatives were purchased from Nacalai Tesque (Kyoto, Japan), Kokusan Chemical Co Ltd. (Tokyo, Japan), Wako Pure Chemical Industries (Osaka, Japan), Bachem AG (Bubendorf, Switzerland), Kanto Chemical (Tokyo, Japan), or Sigma-Aldrich Japan (Tokyo, Japan). Ac-dipeptide-NH_2 compounds were previously synthesized and reported.[23,31] Trp-Ala-Val-NH_2 was newly synthesized by solution-phase techniques.[31] The structure of the peptide was confirmed by high-resolution electron bombardment ionization mass spectrometry [m/z [MH^+]: calcd for $C_{19}H_{27}N_5O_3$, 373.2114; Found, 373.2103 ($\pm$0.0014)]. Lecithin from egg yolk was purchased from Katayama Chemical Industries (Osaka, Japan). Hydrophobic filter plates (MultiScreen-IP, Clear Plates, 0.45 μm-diameter pore size) and 96-well microplates (COSTAR UV-plate) were obtained from Millipore (MA, USA) and Corning (MA, USA), respectively. All other reagents were of analytical grade and were purchased from Wako Pure Chemical Industries or Nacalai Tesque.

5.2. Permeability experiments with artificial membranes

Permeability experiments were carried out in 96-well microplates. A 96-well microplate (acceptor compartment) was completely filled with Tris–HCl buffer (pH 7.3) or sodium phosphate buffer (pH 6.3) containing

5% DMSO. A hydrophobic filter plate (donor compartment) was fixed on the buffer-filled plate. The filter surface was impregnated with 5 μL of 10% (v/v) lecithin solution in 1,9-decadiene. A 200-μL sample of 200–500 μM compound solution in the same buffer containing 5% DMSO was added to the filter plate and incubated at 25 °C for 2, 5 or 24 h. The filter plate was carefully removed. Then, the concentration of the solution in the acceptor compartment was determined by UV spectroscopy, using the microtiter plate reader (Molecular Devices, spectra MAX 250) at 280 nm. A reference solution defining equilibrium conditions was prepared at the same concentration as the sample solution with no membrane barrier. The filter surface was wetted with 5 μL of a 60% (v/v) methanol/buffer solution for the reference. The permeability coefficient through the artificial membrane, $P_{\text{app-pampa}}$ was calculated using eq 7.[27]

$$P_{\text{app-pampa}} = -V_D V_R/[(V_D + V_R)At]\cdot\ln(1 - OD_{\text{sam}}/OD_{\text{ref}}) \quad (7)$$

In this equation, V_D (cm^3) is the donor volume (0.2 cm^3), V_R (cm^3) is the volume of the acceptor compartment (0.38 cm^3), A (cm^2) is the accessible filter area (0.283 cm^2), and t (s) is the incubation time. OD_{sam} and OD_{ref} are the optical density (OD) at 280 nm of the sample and reference solutions in the acceptor compartment, respectively.

5.3. Measurement of the partition coefficient P_{oct}

The partition coefficient P_{oct} (defined for the neutral or non-ionized form) of X-Trp-NH_2, Trp-Ala-Val-NH_2, Ac-D-Trp-Val-NH_2, cyclo(Trp-X), tryptophol, and indole-3-acetamide in the 1-octanol/water system were measured at 25 ± 3 °C by the flask-shaking procedure. The log P_{oct} value of the compounds taking the neutral form at pH 7 [cyclo(Trp-X), tryptophol, and indole-3-acetamide] was obtained with 1-octanol and 0.1 M aqueous sodium phosphate/phosphoric acid (pH 7; ionic strength: 0.1) as the partitioning solvents under the same experimental conditions as reported before.[32] The log P_{oct} value of the basic X-Trp-NH_2 and Trp-Ala-Val-NH_2 was measured using 0.1 N NaOH (pH 13) as the aqueous phase. After the partitioning equilibrium was established, the concentration of compounds in the aqueous phase was measured by their UV absorbance (Shimadzu UV-1600PC). The concentration in the 1-octanol phase was taken as the difference. The measurement was repeated four times for the log P_{oct} values. The standard deviation of both values was mostly within ±0.05. The P_{oct} values are listed in Table 1.

The log P_{oct} values of Trp derivatives, Ac-Trp-Val-NH_2, and Ac-Tyr-X-NH_2 were previously reported.[30,31] For the log P_{oct} value of indole compounds except tryptophol, and indole-3-acetamide, the measured values in the database of the MacLogP software, ver. 4.0[33,34] were used.

5.4. Hydrophobicity parameters

Eqs 8 and 9 represent the relationship between log D_{oct} at a particular pH and log P_{oct} for acids and bases, respectively, if the partition of ion-pair complexes can be neglected.[35]

$$\text{For acids:}\quad \log D_{\text{oct}} = \log P_{\text{oct}} - \text{pH} - \log(K_a + [H^+]) \quad (8)$$

$$\text{For bases:}\quad \log D_{\text{oct}} = \log P_{\text{oct}} - \text{p}K_a - \log(K_a + [H^+]) \quad (9)$$

$[H^+]$ is the hydrogen ion concentration of the aqueous phase. According to eqs 8 and 9, log D_{oct} = log P_{oct} for acids when pH << pK_a and for bases when pH >> pK_a (K_a: the acid dissociation constant of the conjugate acids). For acids, when pH >> pK_a, [log D_{oct} = log P_{oct} + pK_a − pH], whereas for bases, when pH << pK_a, [log D_{oct} = log P_{oct} − pK_a + pH]. These equations are unified to one, eq 10.

$$\log D_{\text{oct}} = \log P_{\text{oct}} \sim |\text{p}K_a - \text{pH}| \quad (10)$$

where $|\text{p}K_a - \text{pH}|$ is the absolute value of the difference between the pK_a value of the compound and the experimental pH. Thus, we used log P_{oct} and $|\text{p}K_a - \text{pH}|$ as the hydrophobicity parameter of compounds in the place of log D_{oct}.

5.5. Molecular modeling

All computations were done with the molecular modeling software package SYBYL, version 6.8.[36] To select initial conformations of compounds, we started from the coordinates of the X-ray crystallographic data for the compound, Trp.[37] The X-ray structure of Trp was fully optimized by the semiempirical molecular orbital method, PM3[38,39] to give relatively stable conformer. Structures of the other compounds were constructed by modifying the energy-optimized structure of Trp. The coordinates of the modified parts of these structures were calculated by use of the SYBYL standard values for bond lengths and angles. A systematic search in SYBYL was applied to all rotatable bonds except χ_1 of the Trp side chain. The χ_1 value was fixed as the same value as that of a Trp stable conformer. The low-energy conformer of each compound that was obtained by a systematic search was then geometry optimized by the Tripos force field. All compounds were modeled in their neutral form.

5.6. Surface area calculations

MOLPROP in SYBYL was used to calculate the surface area occupied by hydrogen-bond acceptor and donor

atoms of each modeled conformer (SA_{HD} and SA_{HA}, respectively). The hydrogen-bond acceptor atoms were defined as the nitrogen and oxygen atoms while the hydrogen-bond donor atoms were defined as the hydrogen atoms attached to these hetero atoms. We also calculated the polar and nonpolar part of the surface area (*PSA* and *NPSA*, respectively) and the fraction of each surface area ($\%SA_{HD}$, $\%SA_{HA}$, $\%PSA$, and $\%NPSA$). However, introduction of these parameters did not improve the statistical quality of classical QSAR equations.

5.7. Classical QSAR

The PAMPA permeability, log $P_{app\text{-}pampa}$, was quantitatively analyzed using the classical QSAR technique. All classical QSAR analyses were done with QREG, version 2.05.[40]

5.8. VolSurf

To describe the 3-D molecular field of the compound, the GRID force field (GRID software, version 18[41]) was used. Four probes (water, DRY, carboxyl oxygen and amide nitrogen) were used to characterize interaction sites around target molecules. Three-dimensional molecular field maps were transformed into 88 descriptors by VolSurf, version 3.07.[1] These descriptors are molecular volume (V), shape (S), surface rugosity (R), molecular weight (MW), size of the hydrophilic (W) and hydrophobic (D) regions, hydrogen-bonding properties (HB) and so on. A more detailed representation of VolSurf descriptors has been presented by Cruciani et al.[28]

The correlation of the PAMPA permeability coefficient with the data matrix was analyzed by the partial least squares (PLS) method.[42] The results of the analysis were expressed as correlation equations with the optimum number of latent variable or component terms, each of which was linear combination of original independent lattice variables. We initially selected the number of compounds in the set as the number of the cross-validation (the leave-one-out method) and then performed the analysis using the optimum number of latent variables which was deduced from the cross-validation tests without actual cross-validation. To derive the best equation, the 56 out of 88 VolSurf descriptors were selected by the FFD variable selection method in VolSurf according to the predictive ability of the model equation with the presence or absence of each descriptor.

Acknowledgements

We are thankful to Dr. Kazuhiro Irie of Graduate School of Agriculture at this university for the mass spectral measurement and Professor Everett Bandman of University of California at Davis for careful reviewing this manuscript. We also thank Drs. Ryo Shimizu and Kazuya Nakao of Tanabe Seiyaku Co., Ltd for their helpful suggestions about permeability experiments with artificial membranes. This study was supported in part by the Takeda Science Foundation.

References and notes

1. Cruciani, G.; Pastor, M.; Guba, W. *Eur. J. Pharm. Sci.* **2000**, *11* (Suppl. 2), S29.
2. Palm, K.; Luthman, K.; Ungell, A.; Strandlund, G.; Artursson, P. *J. Pharm. Sci.* **1996**, *85*, 32.
3. Yoshida, F.; Topliss, J. G. *J. Med. Chem.* **2000**, *43*, 2575.
4. Kobayashi, M.; Sada, N.; Sugawara, M.; Iseki, K.; Miyazaki, K. *Int. J. Pharm.* **2001**, *221*, 87.
5. Lipinski, C. A.; Lombardo, F.; Dominy, B. W.; Feeney, P. J. *Adv. Drug Deliv. Rev.* **1997**, *23*, 3.
6. Pidgeon, C.; Ong, S.; Liu, H.; Qiu, X.; Pidgeon, M.; Dantzig, A. H.; Munroe, J.; Hornback, W. J.; Kasher, J. S.; Glunz, L.; Szczerba, T. *J. Med. Chem.* **1995**, *38*, 590.
7. Goodwin, J. T.; Mao, B.; Conradi, R. A.; Burton, P. S. *J. Peptide Res.* **1999**, *53*, 355.
8. Ren, S.; Lien, E. J. *Prog. Drug Res.* **1999**, *54*, 1.
9. Stevenson, C. L.; Augustijins, P. F.; Hendren, R. W. *Int. J. Pharm.* **1999**, *177*, 103.
10. Sternberg, P.; Norinder, U.; Luthman, K.; Artursson, P. *J. Med. Chem.* **2001**, *44*, 1927.
11. Ekins, S.; Durst, G. L.; Stratford, R. E.; Thorner, D. A.; Lewis, R.; Loncharich, R. J.; Wikel, J. H. *J. Chem. Inf. Comput. Sci.* **2001**, *41*, 1578.
12. Fujiwara, S.; Yamashita, F.; Hashida, M. *Int. J. Pharm.* **2002**, *237*, 95.
13. Kulkarni, A.; Han, Y.; Hopfinger, A. J. *J. Chem. Inf. Comput. Sci.* **2002**, *42*, 331.
14. Waterbeemd, H.van de; Camenisch, G. *Quant. Struct.-Act. Relatsh.* **1996**, *15*, 480.
15. Wessel, M. D.; Jurs, P. C.; Tolan, J. W.; Muskal, S. M. *J. Chem. Inf. Comput. Sci.* **1998**, *38*, 726.
16. Alifrangis, L. H.; Christensen, I. T.; Berglund, A.; Sandberg, M.; Hovgaard, L.; Frokjaer, S. *J. Med. Chem.* **2000**, *43*, 103.
17. Yazdanian, M.; Glynn, S. L.; Wright, J. L.; Hawi, A. *Pharm. Res.* **1998**, *15*, 1490.
18. Zhu, C.; Jiang, L.; Chen, T.; Hwang, K. *Eur. J. Med. Chem.* **2002**, *37*, 399.
19. Hirono, S.; Nakagome, I.; Hirano, H.; Matsushita, Y.; Yoshii, F.; Moriguchi, I. *Biol. Pharm. Bull.* **1994**, *17*, 306.
20. Artursson, P.; Karlsson, J. *Biochem. Biophys. Res. Commun.* **1991**, *175*, 880.
21. Sekine, T.; Watanabe, N.; Hosoyamada, M.; Kanai, Y.; Endou, H. *J. Biol. Chem.* **1997**, *272*, 18526.
22. Ueda, K.; Cornwell, M. M.; Gottesman, M. M.; Pastan, I.; Roninson, I. B.; Ling, V.; Riordan, J. R. *Biochem. Biophys. Res. Commun.* **1986**, *141*, 956.
23. Ano, R.; Kimura, Y.; Urakami, M.; Shima, M.; Matsuno, R.; Ueno, T.; Akamatsu, M. *Bioorg. Med. Chem* **2004**, *12*, in press.
24. Kansy, M.; Senner, F.; Gubernator, K. *J. Med. Chem.* **1998**, *41*, 237.
25. Sugano, K.; Hamada, H.; Machida, M.; Ushio, H. *J. Biomol. Screen.* **2001**, *6*, 189.
26. Sugano, K.; Takata, N.; Machida, M.; Saitoh, K.; Terada, K. *Int. J. Pharm.* **2002**, *241*, 241.
27. Wohnsland, F.; Faller, B. *J. Med. Chem.* **2001**, *44*, 923.
28. Cruciani, G.; Crivori, P.; Carrupt, P.-A.; Testa, B. *J. Mol. Struct. (Theochem)* **2000**, *503*, 17.
29. Fujita, T.; Nishioka, T.; Nakajima, M. *J. Med. Chem.* **1977**, *20*, 1071.
30. Urakami, M.; Ano, R.; Kimura, Y.; Shima, M.; Matsuno, R.; Ueno, T.; Akamatsu, M. *Z. Naturforsch.* **2002**, *58c*, 135.
31. Akamatsu, M.; Okutani, S.; Nakao, K.; Hong, N. J.; Fujita, T. *Quant. Struct.-Act. Relat.* **1990**, *9*, 189.
32. Akamatsu, M.; Yoshida, Y.; Nakamura, H.; Asao, M.; Iwamura, H.; Fujita, T. *Quant. Struct.-Act. Relat.* **1989**, *8*, 195.

33. Hansch, C.; Leo, A. In *Exploring QSAR*; American Chemical Society: Washington, DC, 1995; p 125.
34. *MacLogP 4.0*; Biobyte Corp.: Claremont, CA, USA.
35. Terada, H.; Kitagawa, K.; Yoshikawa, Y.; Fujita, T. *Chem. Pharm. Bull.* **1981**, *29*, 7.
36. *SYBYL Molecular Modeling Software*; Tripos Associates, Inc.: St Louis, MO, USA.
37. *The Cambridge Structural Database*; CCSD: Cambridge, UK.
38. Stewart, J. J. P., *MOPAC Ver. 5*; Quantum Chemistry Program Exchange, Program 455: Indiana University, Bloomington, IN.
39. Stewart, J. J. P. *J. Comput. Chem.* **1989**, *10*, 221.
40. Asao, M.; Shimizu, R.; Nakao, K.; Nishioka, T.; Fujita, T. *QREG 2.05*; Japan Chemistry Program Exchange: Ibaraki, Japan.
41. Goodford, P. J. *J. Med. Chem.* **1985**, *28*, 849.
42. Wold, S.; Ruhe, A.; Wold, H.; Dunn, W. J., III *SIAM J. Sci. Stat. Comput.* **1984**, *5*, 735.
43. Kortum, G.; Vogel, W.; Andrussow, K. In *Dissociation Constants of Organic Acids in Aqueous Solution*; Butterworths: London, 1961.
44. Perrin, D. D. In *Dissociation Constants of Organic Bases in Aqueous Solution*; Butterworths: London, 1965.